The Calculation of Light Element Impurity (α,n) Yield Curves in a PuO_2 Matrix and Associated Specific Yield Coefficients: Influence of the Reaction Cross Sections

Stephen Croft[1], Robert D. McElroy Jr.[2], and Andrea Favalli[3,4]

[1]Lancaster University, Bailrigg, Lancaster, UK
[2]Oak Ridge National Laboratory, Oak Ridge, TN, USA
[3]European Commission, Joint Research Centre (JRC), Ispra, Italy
[4]Los Alamos National Laboratory, P.O. Box 1663, Los Alamos, NM 87545, USA

ABSTRACT

Most of the Pu separated from irradiated commercial nuclear fuel is stored as PuO_2. The primary quantitative nondestructive measurement technique used to verify the amount of Pu in storage containers is passive neutron correlation counting. An important physical property of the oxide material is the ratio, α, of the rate of (α,n) neutrons produced inside the item to the rate of neutrons produced by spontaneous fission. This ratio influences the precision of the correlated counting method and affects the interpretation of the data because of how it changes both the primary total neutron production rate and the rate of induced fission events taking place inside the item. In addition to the main O(α,n) contribution, additional contributions come from α-particle interactions with light element impurities that are inevitably present. In this work, we calculate specific (α,n) yield coefficients, expressed in units of neutrons per second per gram of α-emitting nuclide per part per million by mass of the specified impurity element distributed in a pure PuO_2 matrix, for some key α-emitting actinides commonly present in reprocessed Pu ($^{238–242}$Pu+^{241}Am). These coefficients are directly applicable to nuclear safeguards verification work in which the α ratio is often calculated from the Pu-isotopic composition and chemical information obtained by other means. They also provide a convenient up-to-date reference set against which values generated by other methods can be compared. Results are presented for impurities with atomic number from 3 to 17 inclusive, plus K and Fe. In most cases, these coefficients are not expected to change by more than 5%–10% at any time in the future. However, as new data become available, changes as large as 20% may be needed for some targets (e.g., F). The present yield calculations are limited by the general shortage of quality experimental total (α,n) reaction cross section data, which, together with unexplained variation between determinations, means that an objective and coherent evaluation is not possible. The situation is even less satisfactory for the partial differential cross section needed to calculate neutron spectra.

Keywords: (α,n) reactions; passive neutron correlation counting; nuclear data for nuclear safeguards

Introduction

Interest in (α,n) reactions has remained strong since 1932 when the neutron was discovered by bombarding Be with α-particles from ^{210}Po [1,2]. There are numerous basic science and technological reasons for this interest including the study of nuclear structure and nuclear reaction theory, the creation of reference neutron sources, as a signature of special nuclear material, astrophysical modeling of the synthesis of elements, the quantification terrestrial production of radionuclide, hot fusion plasma diagnostics, and dosimetry of vitrified high-level radioactive waste [3,4,5]. In the present work, we focus on just one practical aspect: prediction of neutron production via (α,n) reactions in PuO_2 arising from interactions with light element impurities. It is important to understand the method and its accuracy in relation to the widely used Pu assay technique of passive neutron correlation counting [6,7,8] in which the total neutron counting rate and various orders of correlated-neutron counting rate are determined. However, in the usual one-speed prompt-fission point-item model, the measurement item is described by three model parameters: the spontaneous fission rate, SF; the leakage self-multiplication factor, M_L; and the (α,n)-to-(SF,n) ratio, α. The neutron efficiency of the detector introduces a fourth model parameter [9]. Therefore, to proceed with the quantitative assay of a particular stream of measurement items, usual assumptions are that the response of the detectors is fixed and known through calibration and that the α-ratio can be calculated from the isotopic composition of the Pu. Therefore, only two unknowns remain to be determined from the two observed rates: SF rate (usually expressed in terms of the equivalent or effective ^{240}Pu mass) and M_L. When calculating the relative (α,n) yield, the oxide is typically assumed to be pure even though light element impurities are always present, and their levels may differ from those present in the reference materials used for instrument calibration and validation [10]. The impurity (α,n) coefficients calculated herein permit the impact of impurities to be simply and conveniently estimated by nondestructive assay practitioners. The impurity coefficients given also provide a reference set for comparison as new experimental data and (α,n) source-term code updates become available.

Method

By definition of the microscopic reaction cross section, the probability of a nuclear interaction with a given target species as the α-particle gradually slows down in a medium, is given by differential relation expressed in Eq. (1) [11]:

$$dY = N \cdot \sigma \cdot dx = N \cdot \sigma \cdot \frac{dE}{\left(\frac{dE}{dx}\right)} \tag{1}$$

where dY is the probability (incremental yield in reactions per α-particle) of a reaction as the α-particle travels an incremental path-length distance dx, N is the number density of target nuclei in the medium, and σ is the microscopic cross section of the target nuclei. We are concerned with the overall (α,n)

neutron-yield and use the natural element value given by $\sigma = \sum f_i \cdot \sigma^{(i)}$, where the summation extends over the number of isotopes, f_i is the atom fraction of isotope i, and $\sigma^{(i)}$ is the microscopic (α,n) reaction cross section of isotope i. Values for σ can be estimated by direct experiment, so an explicit summation is not needed, even for elements with multiple isotopes. The (kinetic) energy loss increment is dE, and $\left(\frac{dE}{dx}\right)$ is the linear stopping power of α-particles in the medium at the average energy that an α-particle has at that point in its path.

Here we consider the average behavior over a large number of α-particle histories, we assume the stopping medium is atomically mixed and the same at all points, and we ignore stochastic fluctuations by interpreting $\left(\frac{dE}{dx}\right)$ to be the average linear stopping power in the continuous slowing down approximation. Although the rate of change of kinetic energy with path length is strictly a negative quantity, we take this into account in our yield calculations by reversing signs wherever needed, so $\left(\frac{dE}{dx}\right)$ is a positive quantity here.

By analogy to the definition of nuclear reaction cross section [11], the energy loss can also be expressed in terms of an atomic stopping cross section, defined by Eq. 2:

$$dE = N_{at} \cdot \bar{\varepsilon} \cdot dx \tag{2}$$

or equivalently by Eq. 3:

$$\left(\frac{dE}{dx}\right) = N_{at} \cdot \bar{\varepsilon} \tag{3}$$

where N_{at} is the total (not just the target) number density of atoms in the stopping medium, and $\bar{\varepsilon}$ is the average stopping power cross section per atom in the stopping medium at the kinetic energy of α-particles corresponding to the point in the slowing-down history.

Combining these two concepts, we obtain the theoretical expression for the differential incremental yield, dY, in terms of basic physical quantities:

$$dY = \left(\frac{N \cdot \sigma}{N_{at} \cdot \bar{\varepsilon}}\right) \cdot dE \tag{4}$$

For a binary compound, $X_{n_1}Z_{n_2}$, in which the element X is the target, element Z is a spectator, and n_1 and n_2 are the number of atoms of *X* and *Z*, in the compound, respectively, this expression simplifies to Eq. (5):

$$dY = \frac{n_1}{(n_1 + n_2)} \cdot \frac{\sigma}{\bar{\varepsilon}} \cdot dE \tag{5}$$

The finite change yield, ΔY_{med}, over a small but finite energy step, in a different compound medium, $X_{m_1}V_{m_2}$, (where the element labelled V and the element labelled by X could in principle be the same in the case of the different compound being a pure element but are different for an actual chemical compound) relative to that in a reference compound medium, ΔY_{ref} , is therefore given by Eq. (6):

$$\Delta Y_{med} = \left[\frac{m_1/(m_1 + m_2)}{n_1/(n_1 + n_2)}\right] \cdot \frac{\bar{\varepsilon}_{ref}}{\bar{\varepsilon}_{med}} \cdot \Delta Y_{ref} \tag{6}$$

Thus, the yield curve, $Y_{med}(E_\alpha) = \sum \Delta Y_{med}$, can be estimated from reference data, $Y_{ref}(E_\alpha)$, tabulated as a function of discrete values of E_α by summing over the finite differences from one starting energy to the next. In our case we use 0.1 MeV spacing to match the selection previously made by West and Sherwood [12].

Note the traditional unit for $\bar{\varepsilon}$ is electron volts per quadrillion atoms per square centimeter (eV/(10^{15} atoms/cm^2), or equivalently 10^{-15} eV·cm^2/atom, which perhaps better emphasizes the quantity's "atomic energy loss cross section" nature). However, these units cancel in the relative formulation, so the coefficient $\left[\frac{m_1/(m_1+m_2)}{n_1/(n_1+n_2)}\right]$ is unitless. Therefore, the units of $Y_{med}(E_\alpha)$ are those of $Y_{ref}(E_\alpha)$ (e.g., neutrons per 10^6 α-particles). In the calculation, the stopping power cross section ratio is generated on the same energy grid as the yield curve, and the average of the values across the step is used to calculate the incremental yield.

Results

Of considerable practical interest in international nuclear safeguards nondestructive assay is the case in which an impurity, such as B, is present at a very low level (i.e., a few ppm) in a nominally pure product compound such as PuO_2. Note that, one part per million, 1 ppm, is numerically equal to 10^{-6} gram per gram of chemical compound and is the commonly used analytical unit in the nuclear safeguards community. The corresponding (α,n)-yield scaling rule, which is based on the assumption that such low impurity concentrations do not influence the slowing down of the α-particles, is given by Eq. (7):

$$\Delta Y_{med} = \left[\frac{N/N_{at}}{n_1/(n_1 + n_2)}\right] \cdot \frac{\bar{\varepsilon}_{ref}}{\bar{\varepsilon}_{med}} \cdot \Delta Y_{ref} \tag{7}$$

where, in this example, n_1, n_2, $\bar{\varepsilon}_{ref}$, and ΔY_{ref} refer to the yield measurements made in the reference binary compound containing B as the sole neutron producer (in the special case that the reference material is the element itself, then, $n_1/(n_1 + n_2) = 1$, because $n_2 = 0$, and $\bar{\varepsilon}_{ref}$ reduces to the elemental value); $\bar{\varepsilon}_{med}$ is the average atomic stopping cross section of the host medium, in this case PuO_2, because the impurity is too dilute to make a significant difference; and N/N_{at} is the ratio of the number of B atoms to the total number of Pu plus O atoms present in the PuO_2 stopping medium. For illustration, for 1 ppm by weight of B in PuO_2, we have Eq. (8):

$$N/N_{at} = \frac{1 \times (1 \times 10^{-6}/A_B)}{3 \times (1/(A_{Pu} + 2 \cdot A_O))} \tag{8}$$

where A_B, A_{Pu}, and A_O are the molar masses of B, Pu, and O, respectively. Note $(A_{Pu} + 2 \cdot A_O)$ is the molar mass of the PuO_2 molecule and so this expression shows the impact of Pu isotopic composition which will be quantified later. This expression assumes Bragg–Kleeman additivity, namely that the α-particle stopping power cross sections of Pu and O are independent of chemical binding effects and act independently [13]. It follows immediately from the obvious three-atom variant of the theoretical expression in the limit that the number of target atoms is small compared with the number of other atoms. To evaluate (N/N_{at}), a value must be selected for the molar mass of Pu, A_{Pu}. For the present purposes, we arbitrarily selected a nominal weapons-grade (WG) Pu with the following (Table 1) isotopic composition in wt % expressed with respect to ^{tot}Pu, that is normalized to 100% over only the Pu isotopes, as is conventional in the nuclear safeguards application.

Table 1. WG Pu isotopic composition as used in this work.

Nuclide	**wt %**
^{238}Pu	0.012
^{239}Pu	93.694
^{240}Pu	5.920
^{241}Pu	0.341
^{242}Pu	0.033
^{241}Am	0.100

This composition corresponds to a molar mass of 239.1208 g/mol when ^{241}Am is incorporated into the distribution and the combined distribution is renormalized. This choice is usual and appropriate when one works gravimetrically because Am is part of the overall mass of the plutonium oxide product. The exact value of molar mass used has no significant impact on practical calculations, because, although it changes slightly with actual Pu-isotopic composition, the number of impurity atoms calculated per molecule of PuO_2 at a given ppm of impurity changes even less. Consider the extreme cases of $^{238}PuO_2$ and $^{240}PuO_2$ with molar masses of around 270 and 272, respectively and which bound heat source and high burnup plutonium. The change in the number of impurity atoms to PuO_2 molecules calculated from a specified ppm values is seen to be of the order of only 1 part in 300, which is small considering the other sources of uncertainty. However, it is straightforward to adjust to a given composition if needed.

Using these scaling rules, the yield curves for the low-Z elements Li, Be, B, C, N, O, F, Na, Mg, Al, Si and Fe were generated when present at a level of 1 ppm in PuO_2. The α-particle line-spectra of $^{238\text{-}242}$Pu and ^{241}Am were then overlaid onto the yield curves to obtain specific neutron production coefficients, (α,n) neutrons per second per ppm of impurity per gram of α-emitting nuclide.

Compilations of (α,n) yield data exist but evaluations do not. Although West and Sherwood [12] list some of the nominally most accurate (less than 2% overall total measurement uncertainty at the 68% confidence interval) measured thick-target yield data (the accuracy in some cases itself being limited by uncertainty in the impurity contribution), the coverage in terms of both energy and materials is not complete when judged against application needs. Therefore, for convenience in the first instance, for the present calculations, we have elected to use the compendium of Heaton et al. [3] as listed. Elemental yield curves are provided by these authors with 0.2 MeV spacing, and we interpolated onto a 0.1 MeV grid (our usual default, chosen to match [12]) assuming power-law behavior between nonzero listed entries:

$$y(E) = y(E_i) \cdot \left(\frac{E}{E_i}\right)^{[ln(y(E_{i+1})/y(E_i))/ln(E_{i+1}/E_i)]} \tag{9}$$

The stopping power cross sections were computed using the code SRIM-2013 [14] also interpolated onto the 0.1 MeV grid. In the case of the elements N, O, and F, which are diatomic gases under normal conditions, solid phase was specified in the SRIM calculations. Stopping power cross sections for Pu (atomic number Z = 94) are not available in SRIM 2013. Therefore, they were estimated from those of Th and U (which differ by 2 units in atomic number) assuming a straightforward Z-dependence over the energy range of the present study (1–10 MeV). The scaling rule adopted in the present work is given by Eq. (10):

$$\varepsilon(94) = \varepsilon(92) + [\varepsilon(92) - \varepsilon(90)] \tag{10}$$

An alternative approach, namely proportionate scaling $\varepsilon(94) = [\varepsilon(92)/\varepsilon(90)] \cdot \varepsilon(92)$, gave numerically similar (within < 0.1 %) results over the entire 1 MeV to 10 MeV range. Therefore, either of these empirical approaches can be considered equivalent for the present purpose. Although it would be desirable to have stopping power data on Pu for nuclear safeguards applications for the present discussion the error introduced by our chosen scaling is not significant in relation to other sources of uncertainty.

The online chart of the nuclides NuDat 2.7, maintained by the National Nuclear Data Center [15] supplied α-decay data (half-lives, emission energies, and intensities). To overlay the discrete α-line spectra onto the yield curves, linear interpolation was applied on the 0.1 MeV grid.

PuO_2 with no impurities

For comparison, the specific yields of the same α-emitters were calculated in pure PuO_2, assuming Pu is a nonparticipatory spectator (negligible (α, n) cross section owing to the high Coulomb barrier), using exactly the same methods but based on the yield curve of UO_2 from West and Sherwood [12] (rather than [3]) and extended to 1.4 MeV as described by Croft et al. [16] (but here using SRIM-2013 stopping data for consistency). The O(α,n) case received especial attention in the past, because of its importance in the passive neutron correlation counting of plutonium oxide product material [16], and we take advantage of that work here. The numerical results are summarized in Table 2. Table 3 gives the corresponding results for pure PuO_2. These can be combined with basic spontaneous fission (SF) nuclear data to calculate the (α,n)/(SF,n) ratio for pure PuO_2 from the isotopic composition. Note, the basic nuclear data used to generate these tables generally does not support more than three significant figures.

Table 2. The specific (α,n) yield coefficients, (n/s/g) of α-emitting nuclide per 1 ppm by mass of the specified impurity element distributed in pure WG PuO_2.

	α-emitter					
Impurity (natural isotopic composition)	^{238}Pu	^{239}Pu	^{240}Pu	^{241}Pu	^{242}Pu	^{241}Am
Li	4.367	0.008296	0.03114	0.000134	0.000207	0.8554
Be	137.9	0.3916	1.4410	0.01341	0.02076	27.25
B	37.29	0.1136	0.4175	0.003993	0.006182	7.387
C	0.2093	0.000539	0.00199	1.747E-05	2.7E-05	0.04128
N	0	0	0	0	0	0
O	0.1145	0.000330	0.001214	1.148E-05	1.78E-05	0.02260
F	16.42	0.04231	0.1561	0.001332	0.002062	3.238
Na	3.175	0.006964	0.02581	0.0001848	0.000286	0.6230
Mg	1.969	0.004490	0.01658	0.0001315	0.000204	0.3861
Al	1.005	0.001876	0.00697	4.644E-05	7.18E-05	0.1962
Si	0.1691	0.000356	0.001318	9.094E-06	1.41E-05	0.03309
Fe	0.000425	9.24E-07	3.41E-06	2.972E-08	4.61E-08	7.99E-05

Table 3. The specific O(α,n) yield, (*n/s/g)* of α-emitting nuclide in pure PuO_2.

	α-emitter					
Target	^{238}Pu	^{239}Pu	^{240}Pu	^{241}Pu	^{242}Pu	^{241}Am
PuO_2	14045	40.10	147.5	1.397	2.163	2776

.

Impurity: F

The F(α,n) reaction is extremely important in the nuclear fuel cycle both as a contaminant and also because it accounts for a large part of the neutron source term in low-enriched U stored as bulk UF_6 [17]. The shape and energy of the yield curve has been reviewed recently [18]. The thick target, integrated over angle, yield curve for F (based on stopping cross sections in solid phase) based on the blending approach described by Croft et al. [18] is shown in Figure 1. For comparison, the yield curve based on the Heaton et al. compendium [3] is also shown. The Heaton et al. compendium [3] contains a convenient set of thick-target (α,n) yields in elements from atomic number 3 to 14 and 26 but excluding 10 in 0.2 MeV steps from 1.0 to 9.8 MeV. Rather than show the full energy range from threshold (~2.36 MeV) to 10 MeV, we have concentrated on the narrower interval needed for the nuclides of natural U (^{234}U, ^{235}U, and ^{238}U), $^{238–242}Pu$ and ^{241}Am, which comprises those of greatest interest in fresh nuclear fuels. The α-particle energy range of concern defined by these α-emitters lies between 3.9 and 5.6 MeV.

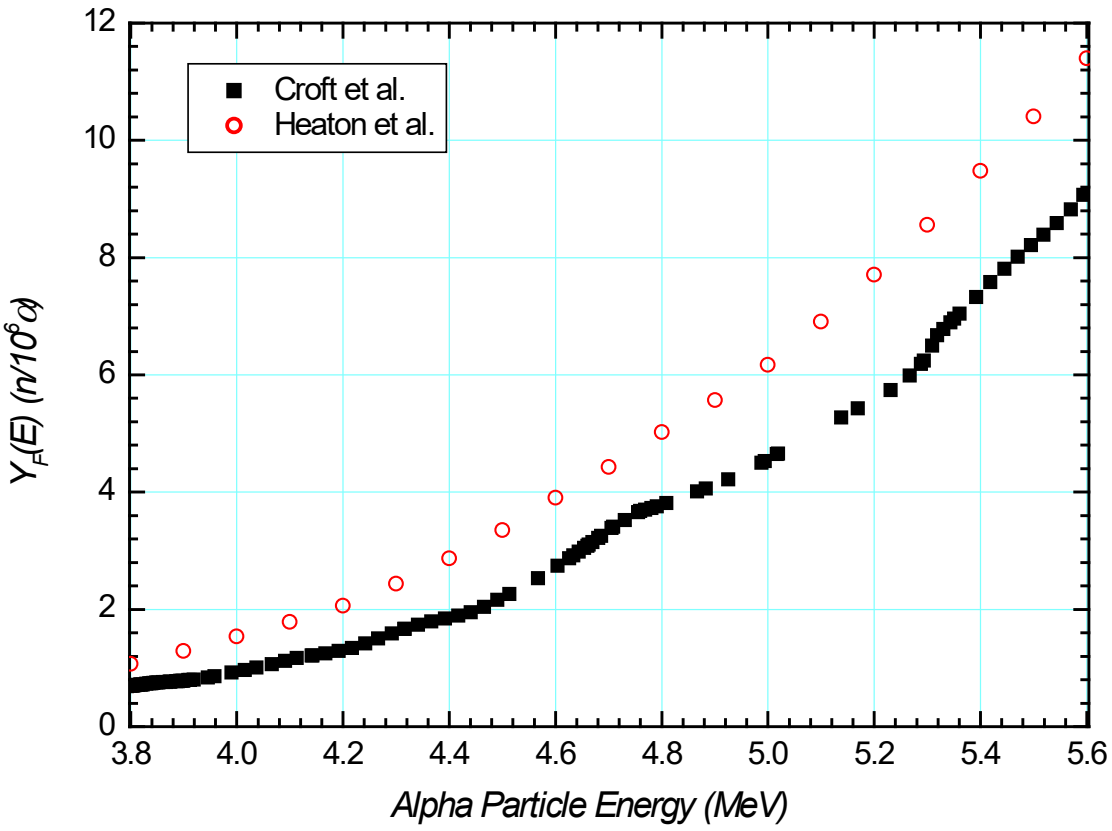

Figure 1. Thick target yield curve, $Y_F(E)$, of elemental fluorine.

The normalization of the curve marked Croft et al. is such that the specific yield of ^{234}U in UF_6 is 510.0 n/s/g. The relatively large difference between the Croft et al. and Heaton et al. curves underscores that the uncertainty in various yield and cross section determinations for the F(α,n) reaction is likely underreported. For this work, ^{234}U was normalized in UF_6, a strategy that emphasizes the energy region around 4.75 MeV where the yield curve in Figure 1 exhibits a kink that presumably also influences the neutron emission spectrum, which affects the detection efficiency of the systems used to collect experimental yield data. Whether normalizing to the 5.5 MeV region using a stochiometric compound of Pu as target, such as PuF_3 or PuF_4, will ultimately prove superior is an open question [19], but it is a technically defensible alternative strategy that in our view merits further experimental and evaluation work by the neutron metrology community. The impurity coefficients for F in PuO_2 based on yield curve of elemental F generated by Croft et al. [18], as outlined here, are summarized in Table 4.

Table 4. The preferred impurity coefficients for F calculated based on the yield curve of Croft et al. [18]. For comparison, the ratio to the higher values obtained using the Heaton et al. compendium [3] are also listed.

α-emitter						
Impurity	^{238}Pu	^{239}Pu	^{240}Pu	^{241}Pu	^{242}Pu	^{241}Am
F	12.95	0.03078	0.1135	0.0009836	0.001522	2.556
Ratio	0.7888	0.7275	0.7268	0.7383	0.7381	0.7893

Impurity: C

The C(α,n) yield has also been the subject of recent critical review not least because ^{13}C(α,n) (the only open channel at the energies of interest here) is important to establishing the inverse reaction ^{16}O(n,α), and it has been used to calibrate the neutron detectors used to make cross section measurements on other targets of astrophysics interest [20]. Again, the question of normalization draws attention because as reaction channels open the neutron emission spectrum shifts, and it is not always clear how this shift will affect the response of the neutron detector. The experiment of West and Sherwood [12] on C and UC targets could monitor and correct for energy spectrum based on the spatial distribution counts in the polyethylene-moderated array of small-diameter low-pressure ^{3}He proportional counters. Compared with [3], they also report on a 0.1 MeV grid (rather than a 0.2 MeV grid) and to four significant figures (rather than three significant figures), but the lowest energy is quite high at about 3.6 MeV for C and 3.8 MeV for UC. Therefore, we extended the yield curve for C reported by West and Sherwood [12] to 2.2 MeV using the Heaton et al. compendium [3] but with a scale factor of 1.037 to match West and Sherwood [12] at 3.6 MeV. The resulting impurity coefficients are listed in Table 5. Also shown is the ratio of these preferred values to those in Table 2. In this case, the agreement is exceptionally good, about 1% difference or less, indicating that the numerical differences between the two approaches exert only a small influence.

Table 5. Impurity coefficients for C, based on West and Sherwood [12] and Heaton et al. [3].

α-emitter						
Impurity	^{238}Pu	^{239}Pu	^{240}Pu	^{241}Pu	^{242}Pu	^{241}Am
C	0.2102	0.000538	0.001987	1.73E-05	2.67E-05	0.04154

Ratio	1.0045	0.9986	0.9989	0.9889	0.9887	1.0064

.

Converting the yield curve data for elemental C to that for UC and comparing it with the impurity-corrected direct measurements reported by West and Sherwood [12] gives good agreement, within about 1.6 % between 3.9 and 5.6 MeV incident energy. This result imparts confidence in both the yield scaling rule and stopping cross section ratios calculated using SRIM-2013. However, above about 7 MeV a systematic gap opens, and the measured UC yield becomes higher by about 9% at 10 MeV. This change, illustrated in Figure 2, is a large and unexpected difference in the context of the experimental accuracy claimed by West and Sherwood [12]. It cannot be explained by the declared possible impurity content of the UC target (based on an analysis of α-induced reaction gamma-rays), and it cannot be a consequence of neutron energy spectrum differences because the same neutron detector is used for both yield curve determinations. Further, it is usual to dismiss any U(α,n) yield as being heavily suppressed by the high Coulomb barrier, although we note that the (α,n) reaction thresholds for ^{234}U, ^{235}U and ^{238}U at 12.81 MeV, 11.08 MeV and 11.48 MeV, respectively, energetically prevent such reactions over the energy range we are discussing.

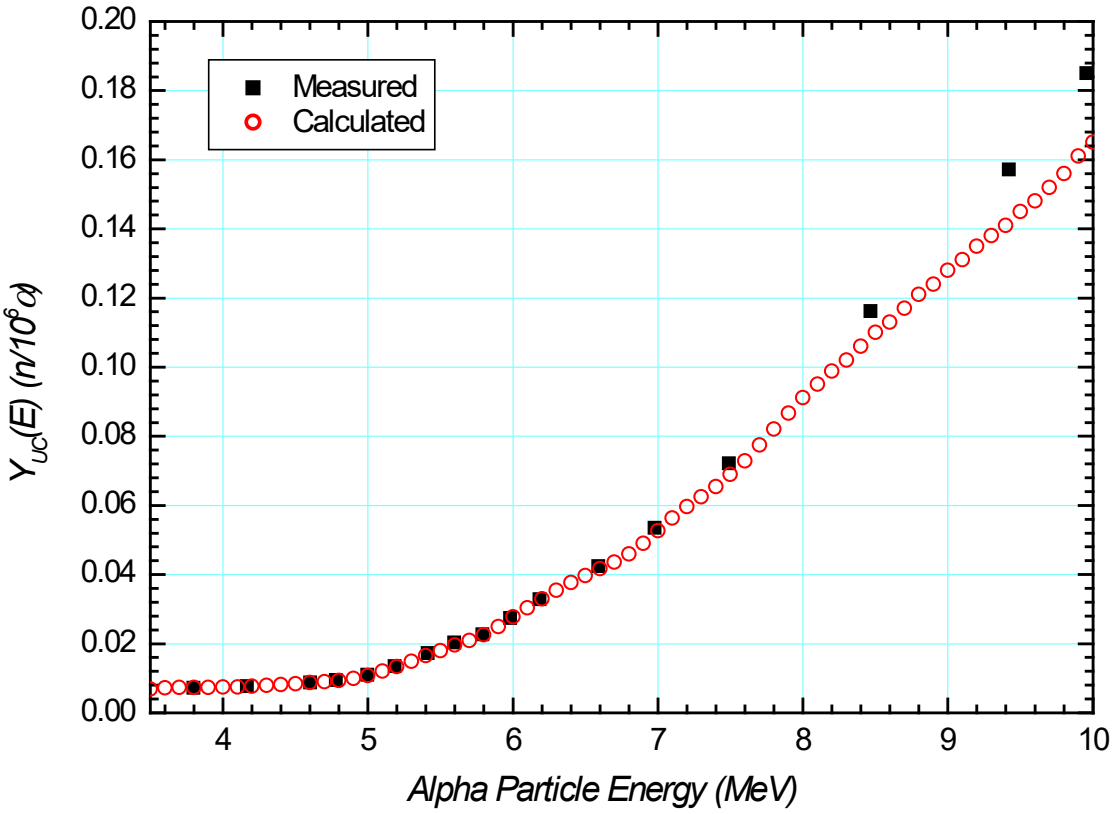

Figure 2. Plot of the thick target integrated over angle yield curve for the compound UC, calculated according to the scaling method described in the text, based on the yield curve measured by West and Sherwood [12] for C. Also shown for comparison is the direct yield curve measured by the same authors for a UC target. Agreement below about 6 MeV is excellent, but the measured yield is systematically larger at higher energies.

Impurity: Mg

In the case Mg(α,n) we also prefer to adopt the yield curve as reported by West and Sherwood [12] but augmented between 1.0 and 3.6 MeV by the data in Heaton et al. [3]. The preferred calculated coefficients and the ratio to those taken from Table 2 are listed in Table 6. Fortunately, the difference is insignificant for the practical work of nuclear materials verification being considered here.

Table 6. Preferred impurity coefficients for Mg calculated using the augmented yield curve of West and Sherwood [12] compared with those based on Heaton et al. [3].

	α-emitter					
Impurity	^{238}Pu	^{239}Pu	^{240}Pu	^{241}Pu	^{242}Pu	^{241}Am
Mg	1.981	0.004495	0.01660	0.000132	0.000204	0.3892
Ratio	1.0063	1.0011	1.0010	1.0024	1.0024	1.0080

In most cases, the uncertainties (represented by the relative standard deviation, RSD) in the preferred coefficients calculated are expected to be on the order of 15% or better. This result is likely to be better than how well the impurity concentrations are known, and therefore may not limit accuracy in practical work at least for the present purposes. However, from a metrology perspective, lower uncertainties than this ought to be technically achievable.

Other impurities: Ne, P, S, Cl, K

As quality data for other elements become available, for instance S [21] or Cl, they can be added to the present collection. For example, Vlaskin et al. [4] is another data compendium that tabulates thick-target (α,n) yield data, in this case from 4 to 9 MeV and for the elements Li to K excluding Ar. Compared with the Heaton et al. compendium [3], this volume adds some information on Ne, P, S, Cl and K, but omits Fe. Although lacking low-energy reach, applying the same calculational procedure to the data compilation of Vlaskin et al. [4], we can estimate specific yield coefficients for these elements to complement those given above. The results are shown in Table 7. Like N, P is energy-forbidden for the α-emitting nuclides considered here. The low-energy yield curves were extrapolated arbitrarily so that the first energy step was not large. However, because the stopping power dependence is weak, and the yield increases steeply with energy, the details of the empirical extrapolation are not important. For Li, C, P, and Cl, we used a quadratic energy dependence; for Ne, S, and K, we used a power law; and for N, we used a combination of the Heaton et al. [3] curve and a quadratic.

Table 7. The specific (α,n) yield coefficients (n/s/g) of α-emitting nuclide per 1 ppm by mass of the specified impurity element distributed in pure WG PuO_2 based on the data compilation of Vlaskin et al. [4].

	α-emitter					
Impurity	^{238}Pu	^{239}Pu	^{240}Pu	^{241}Pu	^{242}Pu	^{241}Am
Li	4.454	0.008639	0.03229	0.0001419	0.0002190	0.87050
Be	136.4	0.3842	1.414	0.01310	0.02028	26.97
B	37.4909	0.113794	0.418225	0.004004004	0.0062	7.434
C	0.21076	0.000523	0.001941	1.76694E-05	2.74E-05	0.04166
N	0	0	0	0	0	0
O	0.123265	0.000357	0.001312	1.243E-05	1.92E-05	0.02434
F	12.38423	0.033758	0.124309	0.001087	0.001682	2.443
Ne	1.682661	0.004312	0.015915	0.0001320	0.000204	0.3316
Na	2.767064	0.005704	0.02119	0.0001638	0.000253	0.5391
Mg	1.940973	0.004405	0.016275	0.0001294	0.000200	0.3813
Al	1.014054	0.001881	0.006992	4.652E-05	7.19E-05	0.1988
Si	0.174531	0.000381	0.001411	9.609E-06	1.49E-05	0.03426
P	0	0	0	0	0	0
S	0.02813	3.38E-05	0.000125	9.312E-07	1.44E-06	0.005500
Cl	0.223071	0.000327	0.001218	4.827E-06	7.43E-06	0.04329
K	0.018564	2.52E-05	9.45E-05	4.160E-07	6.41E-07	0.003584

When the Heaton et al. [3] and Vlaskin et al. [4] compilations overlap, it is instructive to compare the derived coefficients: Table 8 lists the ratio of Vlaskin coefficients to Heaton coefficients. The general agreement is rather good (of course they are not wholly independent because they are based on much the same experimental data). For the present narrow purpose of impurity (α,n) estimation, either data set seems reasonable given the likely uncertainties in the analytical knowledge of the impurity content. Nonetheless, this finding is encouraging because these two authors made independent choices on how to select and normalize the available experimental data generated by the different groups. We have commented on the case of fluorine in detail in the text and therefore elected to use our coefficients. The difference for sodium is down to a nontrivial choice of normalization. We have elected to use the Heaton et al. coefficient, although additional measurements would be welcomed. The difference for O was not expected. Vlaskin et al. [4] remark without providing any supporting detail that it may be something to do with allowing for U(α,n) neutrons, but we do not believe this to be an issue for the reasons already discussed. Therefore, for O we also adopt the coefficients estimated in the present work. These were obtained from those calculated for pure PuO_2, noting that the weight fraction of O in PuO_2 is 118,025 ppm. The ppm coefficient is obtained by dividing the compound coefficient by this factor.

Table 8. Comparison of derived coefficients by way of the ratio (Vlaskin et al./Heaton et al.).

	α-emitter					
Impurity	^{238}Pu	^{239}Pu	^{240}Pu	^{241}Pu	^{242}Pu	^{241}Am
Li	1.0199	1.0414	1.0367	1.0588	1.0585	1.0177
Be	0.98969	0.9811	0.9813	0.9765	0.9765	0.9898
B	1.00529	1.0021	1.0018	1.0028	1.0028	1.0064
C	1.0070	0.9702	0.9755	1.0117	1.0123	1.0094
O	1.0767	1.0809	1.0806	1.0821	1.0821	1.0767
F	0.7542	0.7978	0.7961	0.8156	0.8157	0.7544
Na	0.8715	0.8191	0.8211	0.8863	0.8868	0.8654
Mg	0.9859	0.9809	0.9818	0.9840	0.9841	0.9875
Al	1.0095	1.0025	1.0032	1.0017	1.0018	1.0134
Si	1.0321	1.0697	1.0704	1.0566	1.0564	1.0354

Table 9 lists the selected coefficients that we have adopted and recommend based on the earlier discussion. Alongside each entry we note which data compilation was used: 'H' denotes Heaton et al.; 'V' denotes Vlaskin et al.; '<H&V>' denotes an average of the two, and 'P' denotes values calculated in the present work as discussed in the text. In the present context no more than 3 4 significant figures should be relied on.

Table 9. Summary of the selected specific (α,n) yield coefficients, (n/s/g) of α-emitting nuclide per 1 ppm by mass of the specified impurity element distributed in the pure WG PuO_2 discussed in the text.

		α-emitter					
Impurity	Data	^{238}Pu	^{239}Pu	^{240}Pu	^{241}Pu	^{242}Pu	^{241}Am
Li	H	4.3674	0.008296	0.03114	0.0001340	0.000207	0.8554
Be	H	137.9	0.3916	1.441	0.01341	0.02076	27.25
B	<H&V>	37.399	0.1137	0.4179	0.003998	0.006191	7.411
C	P	0.21029	0.000538	0.001987	1.727E-05	2.67E-05	0.04154
N	H	0	0	0	0	0	0
O	P	0.1190	0.00034	0.001249	1.1837E-05	1.83E-05	0.02352
F	P	12.95	0.03078	0.1135	0.0009836	0.001522	2.556
Ne	V	1.683	0.004312	0.01592	0.00013203	0.000204	0.3316
Na	H	3.175	0.006964	0.02581	0.0001848	0.000286	0.6230
Mg	P	1.9810	0.004495	0.01660	0.0001318	0.000204	0.3892
Al	H	1.0045	0.001876	0.006970	4.644E-05	7.18E-05	0.1962
Si	<H&V>	0.1718	0.000368	0.001364	9.351E-06	1.45E-05	0.03367
P	V	0	0	0	0	0	0
S	V	0.02813	3.38E-05	0.000125	9.312E-07	1.44E-06	0.005500
Cl	V	0.2231	0.000327	0.001218	4.827E-06	7.43E-06	0.04329
K	V	0.01856	2.52E-05	9.45E-05	4.160E-07	6.41E-07	0.003583
Fe	H	0.000425	9.24E-07	3.41E-06	2.972E-08	4.61E-08	7.988E-05

To numerically illustrate a potential application of the recommended coefficients given in Table 9, consider the case in which the nominal WG PuO_2 used to fabricate physical reference standards for calibration of nondestructive assay instruments is contaminated with the light element impurities Li, Be, B, C, N, O, F, Ne, Na, Mg, Al, Si, P, S, Cl, K, and Fe at part per million by weight amounts as shown in Table 10 which is based on an actual case. Note a value of zero for O corresponds to the stoichiometric case PuO_2 (i.e., no extra O is present). The corresponding neutron production rates in neutrons per second per gram of ^{tot}Pu present are also indicated. The total contribution from the impurities is about 3.26 n/s/g ^{tot}Pu in comparison to the value of approximately 50.8 n/s/g ^{tot}Pu calculated for the O(α,n) contribution. Therefore, the impurity (α,n) enhancement is about 6.4 % in this example.

Table 10. Impurity analysis.

Impurity	ppm	^{tot}Pu (n/s/g)
Li	1.2	0.01320
Be	0.3	0.1488
B	7	1.0021
C	260	0.1791
N	45	0
O	0	0
F	10	0.3967
Ne	0	0
Na	100	0.9057
Mg	60	0.3493
Al	90	0.2239
Si	45	0.02161
P	75	0
S	100	0.004800
Cl	20	0.008980
K	35	0.001224
Fe	240	0.0002877

Discussion and remarks

The Passive Nondestructive Assay of Nuclear Material text book is a highly influential teaching aid and a popular practitioner's guidebook, affectionally known as the PANDA manual [5]. In this volume, Norbert Ensslin outlines an approximate way to estimate the relative impurity (α,n) yield in PuO_2 from thick-target elemental values at 5.2 MeV [22]. Norbert was a pioneer in the development and deployment of neutron correlation counting techniques and his outstanding work has been truly inspirational. The present work, which benefits from tools and data not available at that the time, is more comprehensive because the energy treatment is more sophisticated and allows for the nuclide-specific α-line spectra. We also offer an expanded list of impurities (N, Ne, P, S, K, and Fe), are more particular in citing where the yield curve data originated, and are explicit in selecting stopping power cross sections. Finally, we provide numerical coefficients and worked examples. Given that nondestructive assay professionals will however routinely turn to the PANDA book for guidance, it is both important as well as interesting to look at the advice offered there and to see how it compares to the present recommendations. According to Eq. (11-7) of the PANDA manual, the neutron yield of an impurity element present at 1 ppm in PuO_2 relative to stoichiometric O(α,n) contribution is given by Eq. (11):

$$\left(\frac{Y_{1ppm}}{Y_{PuO_2}}\right) \approx \frac{\left(\frac{P_i S_i}{A_i}\right)}{\left(\frac{P_O I_O S_O}{A_O}\right)} \tag{11}$$

In this expression, P_i is the (α,n) yield in the impurity element at 5.2 MeV; $P_O = 0.059$ is the corresponding value for Pu α-particles in units of n/10^6 α-particles; A_i is the molar mass of the impurity element with $A_O = 16$ g/mol being the value for O; $I_O = 118{,}000$ ppm is the concentration of O present in PuO_2; and finally, S_i and S_O are the stopping power cross sections of the impurity element and O, respectively.

Unfortunately, Ensslin does not discuss how the S-values are obtained but refers to Anderson and Lemming [23] for some values. Anderson and Lemming do not explain how the S-values are selected either, but they do list some values for Li, Be, B, O, F, and Al without clear origin (it seems likely they are rooted in the tabulation of Northcliffe and Schilling [24] because although not cited in the text this article is included in their reference list). Northcliffe and Schilling's linear stopping power data cover a broad range of ions, stopping materials, and energy but only with crude resolution (atomic number and energy). Estimating the stopping power cross section values needed for the present calculations requires considerable interpolation. Therefore, based on Ensslin's direction to Anderson and Lemming, and in light of the ambiguities already noted as to how they generated the S-values listed, we decided, for the present illustration, to compute the S_i/S_O values for Li, Be, B, O, F, and Al based directly on the data listed in Anderson and Lemming. For C, Na, Mg, Si, and Cl, we interpolated by fitting a quadratic as a function of atomic number. For completeness, the parameters used here for the Ensslin scaling prescription are listed in Table 11. Using the parameters given in Table 11, we computed the relative impurity (α,n) yields according to the approximate treatment outlined by Ensslin. The results are shown in Table 12. Also listed are the corresponding values calculated by α-emitter using the recommended results (Table 9 and Table 3) of the present work. The general agreement of the approximate treatment with the current detailed calculations is fair in some cases but is factors of several out in others. Additionally, the approximate treatment in the PANDA manual does not capture the significant differences between α-emitters.

Table 11. Parameters adopted in the Ensslin prescription for estimating the relative impurity (α,n) production in PuO_2. The fractional uncertainties given for the P values are based on Ensslin's indicated spread in the values between experimental values that were used to estimate the P-values listed. The S_i/S_O values are given to spurious accuracy because they are based on the ratio of numbers given to only three significant figures.

Impurity	$\boldsymbol{P}$ **(n/10^6 α)**	**Uncertainty (%)**	**A (g/mol)**	$\boldsymbol{S_i/S_O}$
Li	1.13	22	6.94	0.3800
Be	65	7.7	9.01	0.5672
B	17.5	2.3	10.81	0.5846
C	.078	5.1	12.01	0.7709
O	.059	3.4	16.00	1.0000

F	5.9	10	19.00	1.0556
Na	1.1	45	22.99	1.1870
Mg	0.89	2.2	24.31	1.2350
Al	0.41	2.4	26.98	1.2667
Si	0.076	3.9	28.09	1.2956
Cl	0.07	57	35.45	1.2982

459

460

461

462

463 Table 12. Comparison of the impurity (α,n) yields for 1 ppm impurity in stoichiometric PuO_2 relative to
464 the O(α,n) contribution. The results of the present work are listed by α-emitting nuclide alongside the
465 generic estimate based on Ensslin's guidance as implemented as described in the text.

Impurity	**^{238}Pu**	**^{239}Pu**	**^{240}Pu**	**^{241}Pu**	**^{242}Pu**	**^{241}Am**	**"Ensslin"**
Li	3.11E-04	2.07E-04	2.11E-04	9.59E-05	9.55E-05	3.08E-04	1.42E-04
Be	9.82E-03	9.77E-03	9.77E-03	9.60E-03	9.60E-03	9.82E-03	9.40E-03
B	2.66E-03	2.83E-03	2.83E-03	2.86E-03	2.86E-03	2.67E-03	2.18E-03
C	1.50E-05	1.34E-05	1.35E-05	1.24E-05	1.24E-05	1.50E-05	1.15E-05
N	0.00E+00	0.00E+00	0.00E+00	0.00E+00	0.00E+00	0.00E+00	
O	8.47E-06	8.47E-06	8.47E-06	8.47E-06	8.47E-06	8.47E-06	8.47E-06
F	9.22E-04	7.68E-04	7.70E-04	7.04E-04	7.04E-04	9.21E-04	7.53E-04
Ne	1.20E-04	1.08E-04	1.08E-04	9.45E-05	9.45E-05	1.19E-04	
Na	2.26E-04	1.74E-04	1.75E-04	1.32E-04	1.32E-04	2.24E-04	1.31E-04
Mg	1.41E-04	1.12E-04	1.13E-04	9.44E-05	9.43E-05	1.40E-04	1.04E-04
Al	7.15E-05	4.68E-05	4.73E-05	3.32E-05	3.32E-05	7.07E-05	4.42E-05
Si	1.22E-05	9.19E-06	9.25E-06	6.69E-06	6.69E-06	1.21E-05	8.06E-06
P	0.00E+00	0.00E+00	0.00E+00	0.00E+00	0.00E+00	0.00E+00	
S	2.00E-06	8.44E-07	8.50E-07	6.67E-07	6.66E-07	1.98E-06	
Cl	1.59E-05	8.17E-06	8.26E-06	3.45E-06	3.43E-06	1.56E-05	5.89E-06
K	1.32E-06	6.27E-07	6.41E-07	2.98E-07	2.96E-07	1.29E-06	
Fe	3.03E-08	2.30E-08	2.31E-08	2.13E-08	2.13E-08	2.88E-08	

466

467 For these reasons the present calculational approach represents a substantial improvement over the
468 approximate method outlined in the PANDA manual. The ambiguity of implementation is removed by
469 providing numerical coefficients. Specifically, Table 9 lists a technically defensible set of specific (α,n)
470 yield coefficients, expressed in units of neutrons per second per gram of α-emitting nuclide per 1 ppm
471 by mass of the specified impurity element homogeneously distributed in a pure WG PuO_2 matrix. These

values are based on current best estimates of basic data and are suitable for use in both domestic and international nuclear safeguards applications. We have provided a numerical example to illustrate this.

In this work, only neutron production rates, not spectra, have been considered. This choice is entirely in the spirit of the one neutron energy group interpretational model currently used by the international nuclear safeguards inspectorates to verify Pu inventories by correlated neutron counting, and is in line with the fact that typically some effort is taken in the design of correlated neutron counters to flatten the response as a function of mean energy. However, spectral differences between the (α,n) reactions and the fission spectra of the various source terms in actual measurement items can also influence the observed counting rates. These influences are measurement item and neutron detection system dependent and thus outside the present scope to quantify.

West and Sherwood [12] measured Be, BeO, BN, C, UC, UO_2, Mg, Al, Si, Fe, and stainless steel with high reported accuracy. Therefore, additional comparisons and checks against existing or anticipated future collections of data are also readily possible.

The coefficients calculated herein are independent of, and based on more current data than, the current version of SOURCES-4C, which is available as part of the US Department of Energy's Oak Ridge National Laboratory SCALE code system [25] and is widely used to predict neutron source terms. Therefore, they can be used as a convenient and technically defensible reference set of coefficients against which values calculated by other means, including a revised version of SOURCES-4C, say, can be compared.

Experimental data on (α,n) reactions of both scientific and technological interest is sparse, especially regarding partial differential cross sections that are needed for the calculation of neutron spectra (not considered here but of interest as the response of assay instruments depends on the spectrum to some degree), and exhibits variation that often far exceeds the claimed uncertainties. The user community would benefit from a concerted effort to generate a comprehensive high-quality experimental database for coherent evaluation.

Acknowledgements

S.C. warmly acknowledges the financial support of Lancaster University and A.F. gratefully acknowledges the support of the Joint Research Centre of the European Commission.

References

1. J. Chadwick, Possible existence of a neutron, Nature Vol.129 No.3252(Feb. 27, 1932)312.

2. J. Chadwick, The existence of a neutron, Proceedings of the Royal Society of London. Series A, Containing Papers of a Mathematical and Physical Character Vol.136 No.860(Jun. 1, 1932)692–708.

3. R. Heaton, H. Lee, P. Skensved, and B.C. Robertson, Neutron production from thick-target (α,n) reactions, Nucl. Instrum. and Meths. in Phys. Res. A276(1989)529–538.

4. G.N. Vlaskin, Yu.S. Khomyakov, and V.I. Bulanenko, Neutron yield of the reaction (α,n) on thick targets comprised of light elements, Atomic Energy 117 (5)(March, 2015) (Russian Original Nov., 2014). https://doi.org/10.1007/s10512-015-9933-5.

5. D. Reilly, N. Ensslin, H. Smith Jr., and S. Kreiner (Eds), Passive Nondestructive assay of nuclear materials, US Nuclear Regulatory Commission report NUREG/CR-5550 (March, 1991). Also known as: Los Alamos National Laboratory report LA-UR-90-732. ISBN 0-16-032724-5.

6. N. Ensslin, Principles of neutron coincidence counting. Chapter 16 In: D. Reilly, N. Ensslin, H. Smith Jr., and S. Kreiner (Eds), Passive Nondestructive assay of nuclear materials, US Nuclear Regulatory Commission report NUREG/CR-5550 (March, 1991). Also known as: Los Alamos National Laboratory report LA-UR-90-732. ISBN 0-16-032724-5.

7. S. Croft, A. Favalli, D.K. Hauck, D. Henzlova, and P.A. Santi, Feynman variance-to-mean in the context of passive neutron coincidence counting, Nucl. Instrum. and Meths. in Phys. Res. A 686(2012)136–144.

8. S. Croft and A. Favalli, Incorporating delayed neutrons into the point-model equations routinely used for neutron coincidence counting in nuclear safeguards, Annals of Nuclear Energy, Volume 99, 2017, 36–39.

9. Favalli, A. Croft, and P. Santi, Point model equations for neutron correlation counting: extension of Böhnel's equations to any order, Nucl. Instrum. Meths. in Phys. Res. A, 795(2015)370–375.

10. S. Croft and P.M.J. Chard, Neutronic characterisation of plutonium oxide reference samples at Harwell, Proceedings of the 15th Annual ESARDA (European Safeguards Research and Development Association) Symposium on Safeguards and Nuclear Material Management, "Augustinianum" Institute, Vatican City, Rome, Italy, May 11–13, 1993. ESARDA 26 EUR 15214 EN (1993)511–519.

11. K.H. Beckurts and K. Wirtz, Neutron Physics, Springer-Verlag Berlin Heidelberg, 1964.

12. D. West and A.C. Sherwood, Measurements of Thick-Target (α,n) Yields from Light Elements, Annals of Nuclear Energy 9(1982)551–557.

13. J.F. Ziegler and J.M. Manoyan, The Stopping of Ions in Compounds, Nucl. Instrum. and Meths. in Phys. Res. B35(1988)215–228.

14. J.F. Ziegler, J.P. Biersack, and M.D. Ziegler, SRIM The Stopping and Range of Ions in Matter – Version 7. (SRIM Co., 2008) ISBN-13: 978-0-9654207-1-6, available from www.SRIM.org.

15. Brookhaven National Laboratory, NNDC, chart of the nuclide database NuDat 2.7 Accessed 8 Sept. 2020. https://www.nndc.bnl.gov/nudat2/ The utility cites the individual evaluations published in Nuclear Data Sheets where the half-life and decay scheme data are taken. For ^{241}Pu we took the half-life to be 14.329 years, as listed on the front page of the NuDat tool.

16. S. Croft and R.D. McElroy Jr., The thick target integrated over angle (α,n) yield curve for U_3O_8 over the energy range from 1.5 MeV to 10 MeV and associated specific (α,n) yields of the uranium isotopes, Proceedings of the 54th Annual Institute of Nuclear Materials Management (INMM) Meeting, Palm Desert, California, July 14–18, 2013.

17. D.P. Broughton, S. Croft, C. Romano, and A. Favalli, Sensitivity of the simulation of passive neutron emission from UF_6 cylinders to the uncertainties in both ^{19}F(α,n) energy spectrum and thick target yield of ^{234}U in UF_6. Nucl. Instrum. and Meths. in Phys. Res. A 1009(2021)165485.

18. S. Croft, M. Pigni, R. Venkataraman, and A. Favalli, Status of (α,n)-reaction data for nuclear safeguards – Paper 189, Proceeding of the 59th Annual Meeting of the Institute of Nuclear Materials Management, Baltimore, Maryland, July 23–26, 2018.

19. S. Croft, L.C-A. Bourva, and C.G. Wilkins, The (α, n) Production Rate in Plutonium Fluoride, 25th Annual Meeting ESARDA (European Safeguards Research and Development Association) Symposium on Safeguards and Nuclear Material Management, Stockholm, Sweden, 13-15 May 2003. EUR 20700 EN (2003) Paper P095. ISBN 92-894-5654-X.

20. S. Croft, A. Favalli, and R.D. McElroy Jr., α-particle Induced Yield of 6.13 MeV γ-rays in Carbon, Nucl. Instrum. and Meths. in Phys. Res. A 1013(2021)165636.

21. S. Croft and R.D. McElroy, The Thick Target (α, n) Production Yield of Sulphur, Proceedings of the 43rd Annual Meeting of the Institute of Nuclear Materials Management, Orlando, Florida, June 23-27 2002. CD ROM © 2002 Documation, LLC. Session G: Tuesday 25th June. Poster Session. Paper #381.

22. N. Ensslin, The origin of neutron radiation, Chapter 11 In: D. Reilly, N. Ensslin, H. Smith Jr., and S. Kreiner (Eds), Passive Nondestructive assay of nuclear materials, US Nuclear Regulatory Commission report NUREG/CR-5550 (March, 1991). Also known as: Los Alamos National

Laboratory report LA-UR-90-732. ISBN 0-16-032724-5. Note that Eqn(11-7) has a typographical error; the stopping power cross section appearing in the denominator should be S_O.

23. M.E. Anderson and J.F. Lemming, Selected measurement data for plutonium and uranium, Mound Laboratory report MLM-3009 (Nov., 1982). Also known as: U.S. International Safeguards Project Office report ISPO-157.

24. L.C. Northcliffe and F.F. Schilling, Range and stopping-power tables for heavy ions, Nuclear Data Tables A7(1970)233-463.

25. B.T. Rearden and M.A. Jessee, (Editors), SCALE Code System. ORNL/TM-2005/39, Version 6.2.3, Oak Ridge National Laboratory, Oak Ridge, Tennessee (2018). Available from the Radiation Safety Information Computational Center as CCC-834. https://www.ornl.gov/scale/scale-manual.